

## Breathing and Twisting: An Investigation of Framework Deformation and Guest Packing in Single Crystals of a Microporous Vanadium Benzenedicarboxylate

Xiqu Wang,<sup>\*,†</sup> Juergen Eckert,<sup>‡</sup> Lumei Liu,<sup>†</sup> and Allan J. Jacobson<sup>\*,†</sup>

<sup>†</sup>Department of Chemistry, University of Houston, Houston, Texas 77204-5003, United States, and <sup>‡</sup>Materials Research Laboratory, University of California, Santa Barbara, California 93106-5121, United States

Received December 15, 2010

The structural details of the compounds vanadium benzenedicarboxylate VO(bdc)·Guest, where the Guests are the absorbed six-ring molecules: benzene, 1,4-cyclohexadiene, 1,3-cyclohexadiene, cyclohexene and cyclohexane, have been determined from single crystal X-ray data. All of the six-ring guest molecules show a high degree of ordering inside the channels of VO(bdc). The interactions between the guests and the host framework are dominated by van der Waals bonding. The six-ring molecules are all packed in two columns in the channels, either in herringbone or close to parallel patterns. The packing changes the space group symmetry of VO(bdc) from *Pnma* to the noncentrosymmetric space group *P2<sub>1</sub>2<sub>1</sub>2<sub>1</sub>*. The VO(bdc) framework deforms to closely adapt to the shape and thickness changes of the double columns of the guest molecules. In addition to the well studied breathing deformation, a twisting deformation mechanism that involves a cooperative rotation of the octahedral chains accompanied by bending of the bdc ligand is apparent in the detailed structural data. More quantitative information on the remarkable flexibility of the VO(bdc) framework was obtained from *ab initio* calculations.

### Introduction

The remarkable progress in the synthesis of inorganic–organic hybrid compounds has greatly enhanced the chemical and structural diversity of crystalline microporous materials and the potential for novel applications. The design of metal–organic open frameworks (MOFs) can take advantage of both the variety of organic linkers and specific physical properties of the inorganic core structural units.<sup>1,2</sup> Relative to conventional inorganic porous solids such as zeolites, hybrid organic–inorganic porous frameworks have the advantage of flexibility upon loading and unloading of guest species. The high flexibility can give rise to tunable adsorption selectivity by using changes in external conditions to adjust pore shapes. Compounds with such properties have been categorized as “third generation” microporous materials.<sup>3</sup>

The dianion of 1,4-benzenedicarboxylic acid is a particularly well studied organic linker. A large number of compounds with high porosity and various pore sizes have been synthesized by using this ligand to connect together metal

oxide units with different dimensionalities.<sup>4–6</sup> Among them, a group of compounds with the general framework formula MX(bdc), first reported by Férey and co-workers, are based on chains of *trans* corner-sharing octahedra MX<sub>2</sub>O<sub>4</sub> (M = V,<sup>7</sup> Cr,<sup>8</sup> Al,<sup>9,10</sup> Fe,<sup>11,12</sup> In,<sup>13</sup> Ga,<sup>14</sup> Mn<sup>15</sup> and X = O, OH, F) cross-linked by 1,4-benzene dicarboxylate. The framework that results contains one-dimensional wide channels. Upon removal or adsorption of guest species inside the channels of the structure, large deformations occur without changes in the topology of the framework. Interesting adsorption properties of several members of the family have attracted great

\*To whom correspondence should be addressed. Tel.: 713-743-2785. Fax: 713-742-2787. E-mail: ajacob@uh.edu (A.J.J.), xiqu.wang@mail.uh.edu (X.W.).

(1) Long, J. R.; Yaghi, O. M. *Chem. Soc. Rev.* **2009**, *38*, 1213–1214.  
(2) Férey, G. *Chem. Soc. Rev.* **2008**, *37*, 191–214.  
(3) Kitagawa, S.; Kitaura, R.; Noro, S.-i. *Angew. Chem., Int. Ed.* **2004**, *43*, 2334–2375.  
(4) Férey, G.; Mellot-Draznieks, C.; Serre, C.; Millange, F.; Dutour, J.; Surble, S.; Margiolaki, I. *Science (Washington, DC)* **2005**, *309*, 2040–2042.

(5) Eddaoudi, M.; Kim, J.; Rosi, N.; Vodak, D.; Wachter, J.; O’Keeffe, M.; Yaghi, O. M. *Science* **2002**, *295*, 469–472.  
(6) Rao, C. N. R.; Cheetham, A. K.; Thirumurugan, A. J. *Phys.: Condens. Matter* **2008**, *20*, 159801/1.  
(7) Barthelet, K.; Marrot, J.; Riou, D.; Férey, G. *Angew. Chem., Int. Ed.* **2002**, *41*, 281–284.  
(8) Serre, C.; Millange, F.; Thouvenot, C.; Nogues, M.; Marsolier, G.; Louer, D.; Férey, G. *J. Am. Chem. Soc.* **2002**, *124*, 13519–26.  
(9) Férey, G.; Latroche, M.; Serre, C.; Millange, F.; Loiseau, T.; Percheron-Guegan, A. *Chem. Commun.* **2003**, 2976–2977.  
(10) Liu, L.; Wang, X.; Jacobson Allan, J. *Dalton Trans* **2010**, *39*, 1722–5.  
(11) Whitfield, T. R.; Wang, X.; Jacobson, A. J. *Mater. Res. Soc. Symp. Proc.* **2002**, *755*, 191–196.  
(12) Whitfield, T. R.; Wang, X.; Liu, L.; Jacobson, A. J. *Solid State Sci.* **2005**, *7*, 1096–1103.  
(13) Anokhina, E.; Vougo-Zanda, M.; Wang, X.; Jacobson Allan, J. *J. Am. Chem. Soc.* **2005**, *127*, 15000–1.  
(14) Vougo-Zanda, M.; Huang, J.; Anokhina, E. V.; Wang, X.; Jacobson Allan, J. *Inorg. Chem.* **2008**, *47*, 11535–42.  
(15) Xu, G.; Zhang, X.; Guo, P.; Pan, C.; Zhang, H.; Wang, C. *J. Am. Chem. Soc.* **2010**, *132*, 3656–3657.

interest because of potential applications including storage of gases such as H<sub>2</sub>, CO<sub>2</sub>, and CH<sub>4</sub>; molecule separations, for example, vapor phase adsorption and separation of xylene isomers; and drug delivery.<sup>16–31</sup> Functional groups of various polarities, hydrophilicities, and acidities were recently introduced through substitution in the framework phenyl groups, and their effects on pore opening and the host–guest interactions were reported.<sup>32–34</sup>

We have reported the synthesis of [VO(bdc)](H<sub>2</sub>bdc)<sub>0.71</sub> (traditionally designated as MIL-47<sup>7</sup>) in the form of large single crystals.<sup>35</sup> After removal of the guest acid molecules by heating the crystals of [VO(bdc)](H<sub>2</sub>bdc)<sub>0.71</sub> in the air, we observed that the VO(bdc) structure is sufficiently flexible to undergo single-crystal-to-single-crystal transformations upon the adsorption of aniline, acetone, thiophene, and other molecules enabling the details of the guest structure, framework–guest interactions, and framework deformations to be determined from single crystal X-ray diffraction data. Furthermore, we have observed the rapid and highly selective adsorption of organic sulfur molecules from methane or

octane by VO(bdc), a process relevant to clean fuels.<sup>36,37</sup> The details of the crystal structures show the importance of noncovalent interactions in determining the guest molecule packing within the nanochannels and are valuable in helping to understand the adsorption properties. Most recently, Leus et al. reported remarkable catalytic activity of VO(bdc) in the epoxidation of cyclohexene.<sup>38</sup>

We have extended our earlier study to other guest molecules with different shapes and chemical bonding possibilities. In the structural study of the VO(bdc) framework loaded with different six-ring organic molecules, a twisting deformation mode accompanied by a cooperative rotation of the octahedral chains and bending of the bdc ligands has been observed. This deformation mode is complementary to the well investigated breathing deformation which corresponds to a cooperative translation of the octahedral chains. In the present work, we show that combinations of the twisting and breathing deformations occur when different molecules are absorbed into the VO(bdc) framework. Quantitative insights into these deformations and the remarkable flexibility of the VO(bdc) framework have been obtained from *ab initio* calculations.

## Experimental Section

Crystalline [VO(bdc)](H<sub>2</sub>bdc)<sub>0.71</sub>, **1**, was synthesized as previously reported.<sup>35</sup> For the adsorption measurements, red prismatic crystals of **1** were heated in the air to 380 °C using a 10 °C min<sup>−1</sup> heat-up rate to remove H<sub>2</sub>bdc and to form VO(bdc), **2**. X-ray diffraction measurements on both powder and single crystal samples after heating confirmed the integrity of the structure of VO(bdc). Adsorption experiments were carried out by immersing crystals of **2** in liquid benzene, 1,4-cyclohexadiene, 1,3-cyclohexadiene, cyclohexene, or cyclohexane in the air at room temperature. After immersing the VO(bdc) crystals in the corresponding guest liquid for ~1 h, a suitable crystal for each intercalation compound was selected and sealed in a capillary in the air together with the guest liquid and mounted on a Bruker Apex-II diffractometer for X-ray data collection. Structure determination and refinements were performed using the Bruker SHELXTL software package.<sup>39</sup> Data collection and structure refinement details are listed in Table 1. Volumes of various voids within the structures are calculated using the program PLATON and the van der Waals radii: C, 1.70 Å; H, 1.20 Å; O, 1.52 Å; V, 2.13 Å.<sup>40</sup>

In order to obtain more quantitative information on the remarkable flexibility of the VO(bdc) framework revealed in our crystallographic studies, we carried out *ab initio* calculations. All energy calculations were performed with the DFT-based code VASP<sup>41–45</sup> using the more recent PAW potentials<sup>46</sup> and the PBE functional.<sup>47</sup> An energy cutoff of

(16) Finsy, V.; Kirschhock, C. E. A.; Vedts, G.; Maes, M.; Alaerts, L.; De Vos, D. E.; Baron, G. V.; Denayer, J. F. M. *Chem.—Eur. J.* **2009**, *15*, 7724–7731.

(17) Alaerts, L.; Maes, M.; Jacobs, P. A.; Denayer, J. F. M.; De Vos, D. E. *Phys. Chem. Chem. Phys.* **2008**, *10*, 2979–2985.

(18) Alaerts, L.; Kirschhock, C. E. A.; Maes, M.; van der Veen, M. A.; Finsy, V.; Depla, A.; Martens, J. A.; Baron, G. V.; Jacobs, P. A.; Denayer, J. F. M.; De Vos, D. E. *Angew. Chem., Int. Ed.* **2007**, *46*, 4293–4297.

(19) Millange, F.; Guillou, N.; Medina, M. E.; Férey, G.; Carlin-Sinclair, A.; Golden, K. M.; Walton, R. I. *Chem. Mater.* **2010**, *22*, 4237–4245.

(20) Rosenbach, N., Jr.; Ghoufi, A.; Deroche, I.; Llewellyn, P. L.; Devic, T.; Bourrelly, S.; Serre, C.; Férey, G.; Maurin, G. *Phys. Chem. Chem. Phys.* **2010**, *12*, 6428–6437.

(21) Salles, F.; Kolokolov, D. I.; Jobic, H.; Maurin, G.; Llewellyn, P. L.; Devic, T.; Serre, C.; Férey, G. *J. Phys. Chem. C* **2009**, *113*, 7802–7812.

(22) Salles, F.; Jobic, H.; Ghoufi, A.; Llewellyn, P. L.; Serre, C.; Bourrelly, S.; Férey, G.; Maurin, G. *Angew. Chem., Int. Ed.* **2009**, *48* (8335–8339), S8335/S–S8335/9.

(23) Hamon, L.; Llewellyn, P. L.; Devic, T.; Ghoufi, A.; Clet, G.; Guillermin, V.; Pirngruber, G. D.; Maurin, G.; Serre, C.; Driver, G.; van Beek, W.; Jolimaite, E.; Vimont, A.; Daturi, M.; Férey, G. *J. Am. Chem. Soc.* **2009**, *131*, 17490–17499.

(24) Hamon, L.; Serre, C.; Devic, T.; Loiseau, T.; Millange, F.; Férey, G.; De Weireld, G. *J. Am. Chem. Soc.* **2009**, *131*, 8775–8777.

(25) Finsy, V.; Ma, L.; Alaerts, L.; De Vos, D. E.; Baron, G. V.; Denayer, J. F. M. *Microporous Mesoporous Mater.* **2009**, *120*, 221–227.

(26) Finsy, V.; Calero, S.; Garcia-Perez, E.; Merklings, P. J.; Vedts, G.; De Vos, D. E.; Baron, G. V.; Denayer, J. F. M. *Phys. Chem. Chem. Phys.* **2009**, *11*, 3515–3521.

(27) Trung, T. K.; Trens, P.; Tanchoux, N.; Bourrelly, S.; Llewellyn, P. L.; Loera-Serna, S.; Serre, C.; Loiseau, T.; Fajula, F.; Férey, G. *J. Am. Chem. Soc.* **2008**, *130*, 16926–16932.

(28) Ramsahye, N. A.; Maurin, G.; Bourrelly, S.; Llewellyn, P. L.; Serre, C.; Loiseau, T.; Devic, T.; Férey, G. *J. Phys. Chem. C* **2008**, *112*, 514–520.

(29) Basu, S.; Maes, M.; Cano-Odena, A.; Alaerts, L.; De Vos, D. E.; Vankelecom, I. F. J. *J. Membr. Sci.* **2009**, *344*, 190–198.

(30) Horcajada, P.; Serre, C.; Maurin, G.; Ramsahye, N. A.; Balas, F.; Vallet-Regi, M.; Sebban, M.; Taulelle, F.; Férey, G. *J. Am. Chem. Soc.* **2008**, *130*, 6774–6780.

(31) Horcajada, P.; Chalati, T.; Serre, C.; Gillet, B.; Sebrie, C.; Baati, T.; Eubank, J. F.; Heurtaux, D.; Clayette, P.; Kreuz, C.; Chang, J.-S.; Hwang, Y. K.; Marsaud, V.; Bories, P.-N.; Cynober, L.; Gil, S.; Férey, G.; Couvreur, P.; Gref, R. *Nat. Mater.* **2010**, *9*, 172–178.

(32) Couck, S.; Denayer, J. F. M.; Baron, G. V.; Remy, T.; Gascon, J.; Kapteijn, F. *J. Am. Chem. Soc.* **2009**, *131*, 6326–6327.

(33) Devic, T.; Horcajada, P.; Serre, C.; Salles, F.; Maurin, G.; Moulin, B.; Heurtaux, D.; Clet, G.; Vimont, A.; Greneche, J.-M.; Le Ouay, B.; Moreau, F.; Magnier, E.; Filinchuk, Y.; Marrot, J.; Lavalley, J.-C.; Daturi, M.; Férey, G. *J. Am. Chem. Soc.* **2010**, *132*, 1127–1136.

(34) Couck, S.; Remy, T.; Baron, G. V.; Gascon, J.; Kapteijn, F.; Denayer, J. F. M. *Phys. Chem. Chem. Phys.* **2010**, *12*, 9413–9418.

(35) Wang, X.; Liu, L.; Jacobson, A. J. *Angew. Chem., Int. Ed.* **2006**, *45*, 6499–6503.

(36) Jacobson, A. J.; Liu, L.; Wang, X. Patent WO 2008021194, 2008.

(37) Liu, L.; Wang, X.; Jacobson, A. J. *J. Mater. Res.* **2009**, *24*, 1901–1905.

(38) Leus, K.; Muylaert, I.; Vandichel, M.; Marin Guy, B.; Waroquier, M.; Van Speybroeck, V.; Van der Voort, P. *Chem Commun* **2010**, *46*, 5085–7.

(39) Sheldrick, G. M. *SHELXTL*; Bruker AXS: Madison, WI, 2005.

(40) Spek, A. L. *PLATON*; Utrecht University: Utrecht, The Netherlands, 2008.

(41) Kresse, G.; Hafner, J. *Phys. Rev. B: Condens. Matter* **1993**, *47*, 558–61.

(42) Kresse, G.; Hafner, J. *Phys. Rev. B: Condens. Matter* **1994**, *49*, 14251–69.

(43) Kresse, G.; Furthmüller, J. *Comput. Mater. Sci.* **1996**, *6*, 15–50.

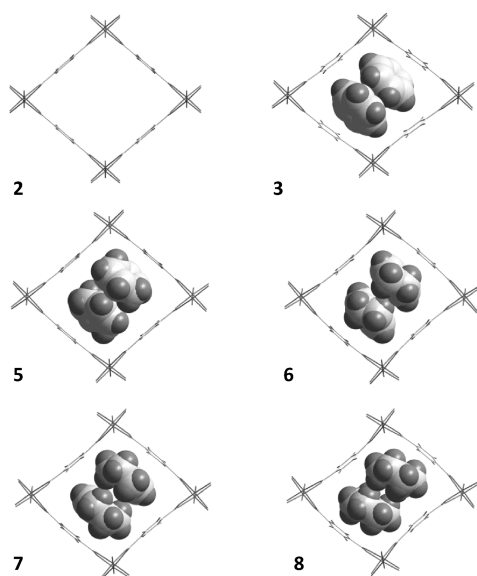
(44) Kresse, G.; Furthmüller, J. *Phys. Rev. B: Condens. Matter* **1996**, *54*, 11169–11186.

(45) VASP group, Theoretical Physics Department, Vienna. <http://cms.mpi.univie.ac.at/vasp/> (accessed Jan 2011).

**Table 1.** Crystal Data and Structure Refinement for [VO(bdc)](benzene)-LT, **3**; [VO(bdc)](benzene)-RT, **4**; [VO(bdc)](1,4-cyclohexadiene), **5**; [VO(bdc)](1,3-cyclohexadiene), **6**; [VO(bdc)](cyclohexene), **7**; and [VO(bdc)](cyclohexane), **8**

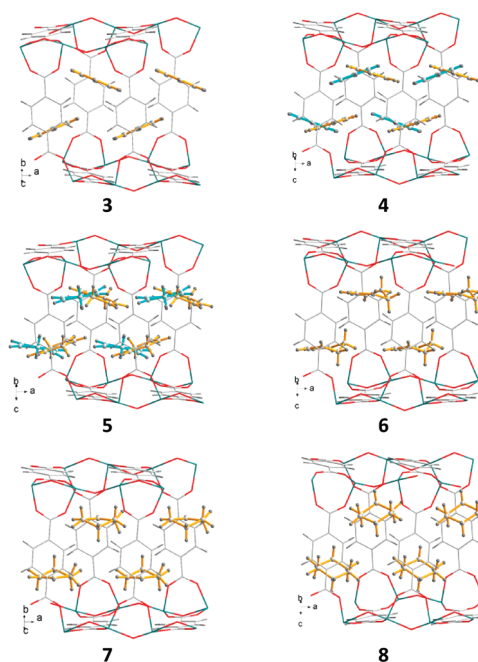
compound	<b>3</b>	<b>4</b>	<b>5</b>	<b>6</b>	<b>7</b>	<b>8</b>
guest	benzene	benzene	1,4-cyclohexadiene	1,3-cyclohexadiene	cyclohexene	cyclohexane
guest/V mol. ratio	0.795(8)	1.0	0.76(2)	1.0	0.81(1)	0.924(4)
formula	C <sub>12.75</sub> H <sub>8.75</sub> O <sub>5</sub> V	C <sub>14</sub> H <sub>10</sub> O <sub>5</sub> V	C <sub>12.72</sub> H <sub>10.29</sub> O <sub>5</sub> V	C <sub>14</sub> H <sub>12</sub> O <sub>5</sub> V	C <sub>13.43</sub> H <sub>13.02</sub> O <sub>5</sub> V	C <sub>13.54</sub> H <sub>15.09</sub> O <sub>5</sub> V
fw	292.89	309.16	294.08	311.18	305.30	308.79
temp/K	223(2)	296(2)	296(2)	296(2)	296(2)	296(2)
wavelength/Å	0.71073	0.71073	0.71073	0.71073	0.71073	0.71073
space group	<i>P</i> 2 <sub>1</sub> 2 <sub>1</sub> 2 <sub>1</sub>	<i>P</i> 2 <sub>1</sub> 2 <sub>1</sub> 2 <sub>1</sub>	<i>P</i> 2 <sub>1</sub> 2 <sub>1</sub> 2 <sub>1</sub>	<i>P</i> 2 <sub>1</sub> 2 <sub>1</sub> 2 <sub>1</sub>	<i>P</i> 2 <sub>1</sub> 2 <sub>1</sub> 2 <sub>1</sub>	<i>P</i> 2 <sub>1</sub> 2 <sub>1</sub> 2 <sub>1</sub>
<i>a</i> /Å	6.7884(7)	6.8018(4)	6.802(1)	6.8050(3)	6.827(8)	6.8127(3)
<i>b</i> /Å	13.231(1)	13.5344(9)	13.912(3)	13.9793(7)	13.965(16)	13.7142(7)
<i>c</i> /Å	16.636(2)	16.416(1)	16.052(3)	15.9447(8)	16.073(18)	16.0701(8)
<i>V</i> /Å <sup>3</sup>	1494.1(3)	1511.2(2)	1519.1(5)	1516.8(1)	1532(3)	1501.44(13)
<i>Z</i>	4	4	4	4	4	4
data/params	3407/170	2558/152	3590/178	3563/181	2355/140	3557/182
goodness-of-fit	1.067	1.057	1.052	1.057	1.071	1.046
R1/wR2 [ <i>I</i> > 2σ( <i>I</i> )] <sup>a</sup>	0.0336/0.0901	0.0282/0.0810	0.0373/0.0994	0.0284/0.0766	0.0535/0.1237	0.0283/0.0765
R1/wR2 [all data] <sup>a</sup>	0.0380/0.0925	0.0301/0.0824	0.0426/0.1022	0.0304/0.0778	0.0913/0.1381	0.0298/0.0772

$$^a R1 = \sum ||F_o| - |F_c|| / \sum |F_o|, wR2 = [\sum (w(F_o^2 - F_c^2)^2) / \sum (wF_o^2)^2]^{1/2}.$$

**Figure 1.** Crystal structure views along channel axis [100] for [VO(bdc)], **2**; [VO(bdc)](benzene)-LT, **3**; [VO(bdc)](1,4-cyclohexadiene), **5**; [VO(bdc)](1,3-cyclohexadiene), **6**; [VO(bdc)](cyclohexene), **7**; and [VO(bdc)](cyclohexane), **8**. Vanadium, oxygen, carbon, and hydrogen atoms are plotted in green, red, gray, and dark gray, respectively.

400 eV for the plane wave basis set was used. We did calculate the relative energies of the empty framework structures with a larger energy cutoff (450 eV) and found that the differences in the relative energies were well within the uncertainties expected for this type of calculation; the energy cutoff did not affect the energetic ordering of the structures. The k-points were generated using a  $2 \times 2 \times 2$  Monkhorst–Pack setting.

In the first step, we performed single-point energy calculations on each of the framework structures using the atomic positions from the single crystal diffraction results for the different guest–host systems by ignoring the guest molecules. C–H bond distances were, however, corrected to the expected value of 1.01 Å because of the well-known foreshortening observed in X-ray diffraction. We also obtained estimates of the host/guest binding energies for selected phases.

**Figure 2.** Structure views along [043] for [VO(bdc)](benzene)-LT, **3**; [VO(bdc)](benzene)-RT, **4**; [VO(bdc)](1,4-cyclohexadiene), **5**; [VO(bdc)](1,3-cyclohexadiene), **6**; [VO(bdc)](cyclohexene), **7**; and [VO(bdc)](cyclohexane), **8**. The two disordered orientations of guest molecules in **4** and **5** are plotted with yellow and blue bonds, respectively.

These are taken to be the difference in the single-point energies (based on experimental crystal structures) of the framework including guests to the sum of energies of the empty framework and the guests themselves (in the configuration found in the framework).

## Results and Discussion

Six host/guest structures [VO(bdc)](benzene)-LT, **3**; [VO(bdc)](benzene)-RT, **4**; [VO(bdc)](1,4-cyclohexadiene), **5**; [VO(bdc)](1,3-cyclohexadiene), **6**; [VO(bdc)](cyclohexene), **7**; and [VO(bdc)](cyclohexane), **8**, were refined from the single crystal data. As shown in Figures 1 and 2, in all six structures, the guest molecules are packed in two columns inside each channel of the VO(bdc) framework. Most noticeably, as the shape of the guest molecules changes from the flat benzene

(46) Kresse, G.; Joubert, D. *Phys. Rev. B: Condens. Matter Mater. Phys.* **1999**, *59*, 1758–1775.

(47) Perdew, J. P.; Burke, K.; Ernzerhof, M. *Phys. Rev. Lett.* **1996**, *77*, 3865–3868.

molecule to the more spherical cyclohexane, the framework deforms through cooperative rotation of the octahedral chains together with progressive bending of the channel walls. When viewed along the channel axis, the deformation appears to be caused by twisting neighboring octahedral chains relative to each other. This “twisting” deformation is in contrast to the well studied breathing deformation in other phases of the MIL-47 and MIL-53 families.<sup>48</sup> A typical example of a breathing deformation is found for [VO(bdc)](acetone) in which the diamond shaped host channels close up substantially by cooperative translation of the octahedral chains upon adsorption of guest acetone molecules, but there is no rotation of the octahedral chains. The V–O–C–C torsion angles of the framework vary like hinges to facilitate the breathing mechanism, and the bdc ligands stay practically flat.<sup>35</sup> Structural details of **3–8** described in the following sections indicate that the “twisting” deformation is mainly a result of adaption of the framework to the space requirements of the guest molecule packing. There is little change observed in the V–O bond lengths after adsorption, indicating that the adsorption of the guest molecules does not change the tetravalent state of the vanadium atoms. The vanadium atoms are tetravalent in all of the compounds (**3–8**) studied.

**The Porous Structure of VO(bdc), 2.** The structure of VO(bdc), **2**, has been briefly described in the literature.<sup>7,35</sup> It contains single chains of VO<sub>6</sub> octahedra cross-linked by bdc ligands. The octahedral chains have a –O=V–O=V– backbone with alternating short and long V–O apical bonds of the VO<sub>6</sub> octahedra and a V–O–V angle of 128.7°. The equatorial corners of the VO<sub>6</sub> octahedra are shared with the bdc ligands. The 1D channels parallel to the octahedral chains have a diamond-shaped cross-section with an aperture of  $\sim 7.6 \times 7.7$  Å. The structure has a space group symmetry of *Pnma* with [100] parallel to the octahedral chains and [010] perpendicular to the plane running through the zigzag –O=V–O=V– backbone. The bdc ligands are flat with their benzene ring plane almost parallel to the channel axis. The angle between the bdc benzene ring and the channel axis is only 3.7°. However, this small inclination of bdc toward the channel axis causes a slight fluctuation of the channel aperture along the channel axis. It also makes individual channels polar but the polarities of neighboring channels are in opposite directions. The angle between the long axis of the bdc ligand and the octahedral chain is 86.6°, less than the 90° angle found in the closely related M(OH)(bdc) structures. The deviation is presumably related to the polar feature of individual octahedral chains of VO(bdc) caused by alternating short and long V–O bonds. These orientation features of the framework bdc play a subtle role in the packing patterns of the absorbed guest molecules and in symmetry changes of the structures upon absorption.

**The Crystal Structure of [VO(bdc)](benzene)-LT, 3.** At 223 K, the absorbed benzene molecules form two columns packed in a herringbone arrangement in each channel of the VO(bdc) framework (Figures 1 and 2). The angle between the benzene ring planes of the two columns is 43.8°. The distance between the centers of neighboring benzene rings in each column is commensurate

with the period of the channel, i.e., 6.788 Å, while the distance from a benzene ring center of one column to a neighboring benzene ring center of the other column is 5.04 Å. In contrast, the shortest distance between the benzene ring center and the center of bdc ligands of the framework is 4.62 Å, which is still much longer than those for typical  $\pi$ – $\pi$  interactions but indicates somewhat stronger interaction between the guest and the host than between the guests. The shortest distances from the benzene hydrogen atoms to the neighboring benzene ring centers of guest benzene and host bdc are 3.30 and 3.01 Å, respectively, indicating very weak CH $\cdots\pi$  interactions. It seems that van der Waals interactions are the dominant forces determining the packing of the benzene molecules inside the channels. The herringbone pattern and similar atom distances are also found in the local structure of crystalline benzene.<sup>49</sup>

The two columns of benzene molecules are oriented roughly perpendicular to one pair of the channel walls and are close to parallel to the other pair. The latter pair is slightly bent toward the outside of the channel, while the former pair is bent toward the inside, presumably due to the space requirement of the guest benzene columns. Such bending of the channel walls facilitates and probably is also strengthened by weak electrostatic interactions between the benzene hydrogen atoms and the oxygen atoms of the framework with CH $\cdots$ O distances in the range 2.90–2.99 Å. Similar interactions have been reported for zeolite/guest systems.<sup>50,51</sup> In addition to bending, the inclination of bdc ligands toward the channel axis increased to 9.0° from the value of 3.7° found in VO(bdc), **2**, and in such a way that a four-column herringbone pattern is formed by the two columns of guest benzene molecules, and the two channel walls closely parallel to them.

The guest benzene molecules in neighboring channels are oriented nearly perpendicular to each other, and the polar axes of their herringbone pattern are in opposite directions. The packing features of the guest benzene molecules are not compatible with the mirror and glide plane symmetry of the initial framework, and the space group of the structure is lowered from centrosymmetric *Pnma* to chiral *P2<sub>1</sub>2<sub>1</sub>2<sub>1</sub>* after absorption. Similar symmetry changes caused by absorbing other molecules have been reported previously<sup>35</sup> and are also observed in structures **4–8**.

The occupancy of the benzene molecules was refined to 0.795(8) per vanadium atom. Therefore, about one-fifth of the guest benzene positions are randomly vacant. The calculated packing density is 173 Å<sup>3</sup> per benzene molecule, assuming a full occupancy of the benzene positions, which is lower than in liquid benzene (148 Å<sup>3</sup>).

**The Crystal Structure of [VO(bdc)](benzene)-RT, 4.** An apparent difference between the room temperature **4** and low temperature **3** structures is the random orientational disorder of the guest benzene molecules in the former (Figure 2). Roughly two-thirds of the benzene molecules in **4** are packed and oriented very similarly to the arrangement

(48) Férey, G.; Serre, C. *Chem. Soc. Rev.* **2009**, 38, 1380–1399.

(49) Bacon, G. E.; Curry, N. A.; Wilson, S. A. *Proc. R. Soc. London, Ser. A* **1964**, 279, 98–110.

(50) Vitale, G.; Mellot, C. F.; Cheetham, A. K. *J. Phys. Chem. B* **1997**, 101, 9886–9891.

(51) Yeom, Y. H.; Kim, A. N.; Kim, Y.; Song, S. H.; Seff, K. *J. Phys. Chem. B* **1998**, 102, 9604.

in **3**, while the remaining one-third are flipped to the opposite direction of the channel axis. The disorder is presumably caused by local structures where the guests in neighboring channels all have the same orientation instead of being related by a  $2_1$  axis. Another possibility is the formation of local structures with parallel packed double columns of benzene rings in individual channels, but the observed distances between the benzene carbon sites are too short (3.17 Å) to favor this possibility. The angle between the two herringbone columns of benzene molecules decreases from 43.7° in **3** to 39.1° and 32.6° in **4** for the orientations with high and low occupancies, respectively, which might be related to the slightly expanded period of the framework along the channel axis and the higher guest content of **4**. The observed atom distances indicate much weaker interactions between the guests and between the guest and host benzene rings in **4** than in **3**. However, the shortest distance between guest benzene hydrogen atoms and the host bridging oxygen atoms is 2.76 Å, shorter than the 2.90 Å observed in **3**.

Compared to **3**, the unit cell volume of **4** increases by 1.1%. The total occupancy of the two orientations of the benzene molecules in **4** was refined very close to 1.0 and was fixed to 1.0 per vanadium atom. The channels of **4** are more open, as indicated by the larger channel diagonal ratio of 13.534/16.417 compared to 13.231/16.636 of **3**, and by the smaller inclination angle of the bdc ligand of 6.2° compared to 9.0° of **3**. The calculated packing density for the guests in **4** is 178 Å<sup>3</sup> per benzene molecule, slightly lower than the low temperature structure **3**.

**The Crystal Structure of [VO(bdc)](1,4-cyclohexadiene), **5**.** The absorbed 1,4-cyclohexadiene molecules are nearly planar with the maximum shift of carbon atoms from the ideal plane less than 0.04 Å, which is closely similar to the planar conformation found in the structure of crystalline 1,4-cyclohexadiene.<sup>52</sup> At room temperature, the 1,4-cyclohexadiene molecules inside the channels of VO(bdc) show a herringbone packing pattern and an orientational disorder similar to the benzene molecules in **4** (Figure 2). One orientation of the guest 1,4-cyclohexadiene molecules has a refined occupancy of 47.1%, for which the angles between the two herringbone columns is 21.4°. The other orientation has a refined occupancy of 28.8% and a much larger angle of 38.6° between the two herringbone columns. The nearest H···C distances between neighboring guest molecules for both orientations are larger than 3.36 Å, indicating mainly intermolecular van der Waals interactions. In contrast, there are relatively short distances (2.92–3.20 Å) from the hydrogen atoms of the guests to the framework carbon atoms. The distances from the hydrogen atoms of the guests to the nearest bridging oxygen atoms of the framework are between 2.75 and 2.79 Å for the two orientations, respectively, indicating relatively strong guest/host interactions.

The channels of **5** are further opened up compared to **4**, as indicated by the larger channel diagonal ratio 13.912/16.052 of **5** compared to 13.534/16.417 of **4**, probably because features of the 1,4-cyclohexadiene molecules are more bulky than the benzene molecules.

**The Crystal Structure of [VO(bdc)](1,3-cyclohexadiene), **6**.** At room temperature, an ordered packing of the absorbed 1,3-cyclohexadiene molecules is observed. As expected, the 1,3-cyclohexadiene molecules have a non-planar conformation, but the butadiene fragment is nearly flat with a C=C–C=C torsion angle of 3.9°.<sup>53</sup> One alkyl carbon atom is above and the other below the butadiene plane. Therefore, the molecule has a twisted wedge shape. The 1,3-cyclohexadiene molecules are packed in two columns in each channel of VO(bdc) with the butadiene fragments almost parallel to each other and to the channel axis (Figure 2). The two columns are shifted relative to each other so that the thick alkyl fragments in one column fit the space near the thin butadiene fragments in the other column. This facilitates a C–H···C=C interaction network between the two columns with relatively short intermolecular distances (C–H···C=C: 2.87–3.04 Å). Relatively strong guest/host interactions are indicated by the short distances from the hydrogen atoms of the guests to the carbon atoms of the framework benzene rings (2.78–2.82 Å), and to the bridging oxygen atoms of the framework (2.87 Å). The former are typical CH··· $\pi$  interactions.<sup>54</sup> The strengthened intermolecular interactions between the guests and between the guest and host may account for the absence of disorder in **6**.

The channel diagonal ratio, 13.98:15.95, of **6** indicates enhanced channel opening compared to **5**. The bending of the channel walls in **6** is more pronounced than in **3–5**, probably because of the increased thickness of the guest molecules. On the other hand, the cell volume of **6** is slightly smaller than that of **5**, due to the stronger interactions between the guests and the host in **6**.

**The Crystal Structure of [VO(bdc)](cyclohexene), **7**.** The conformation of the absorbed cyclohexene molecules is a half-chair with a twist angle of 52.5°. The half-chair conformation of cyclohexene with twist angles close to 60° occurs exclusively in many other crystal structures and is consistent with results from quantum chemical calculations.<sup>55,56</sup> The cyclohexene molecules are packed in two columns related to each other by a 2-fold screw axis in each channel of VO(bdc) (Figure 2). The shortest intermolecular H···C distances between the guests is 3.48 Å, indicating no significant bonding other than van der Waals interactions. However, the packing of the guests seems to fill space most efficiently with the chair backs of one column fitting the double bond part of the other column. Similar to **5** and **6**, relatively strong guest/host interactions are indicated by the short distances from the hydrogen atoms of the cyclohexene molecules to the carbon atoms of the framework (2.90–3.23 Å) and to the bridging oxygen atoms of the framework (2.99 Å).

The occupancy of the cyclohexene molecule was refined to 0.81(1), rather close to the guest occupancies in **3** and **5**. The channel opening and the bending of the channel walls in **7** are both slightly decreased compared to **6** in spite of the large molecule size and the large intermolecular distances of

(53) Shishkin, O. V. *J. Struct. Chem.* **2000**, *41*, 383–387.

(54) Suezawa, H.; Yoshida, T.; Umezawa, Y.; Tsuboyama, S.; Nishio, M. *Eur. J. Inorg. Chem.* **2002**, 3148–3155.

(55) Shishkina, S. V.; Shishkin, O. V.; Leszczynski, J. *Chem. Phys. Lett.* **2002**, *354*, 428–434.

(56) Ibberson, R. M.; Telling, M. T. F.; Parsons, S. *Cryst. Growth Des.* **2008**, *8*, 512–518.

(52) Jeffrey, G. A.; Buschmann, J.; Lehmann, C. W.; Luger, P. *J. Am. Chem. Soc.* **1988**, *110*, 7218–19.

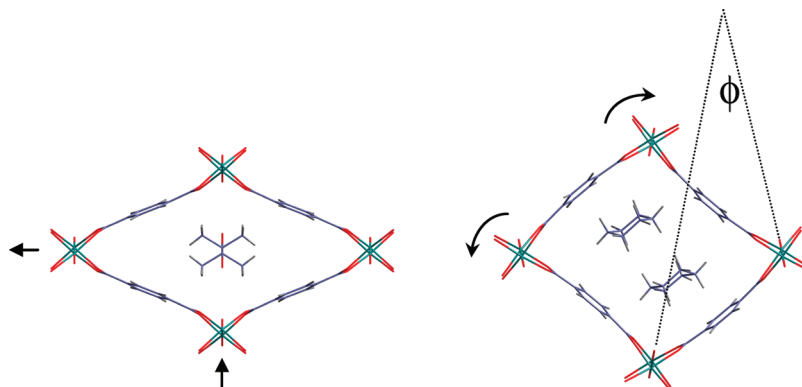


**Figure 3.** The “breathing” (left) and the “twisting” (right) deformation mode of the VO(bdc) framework. The angle  $\phi$  is a measure of twisting.

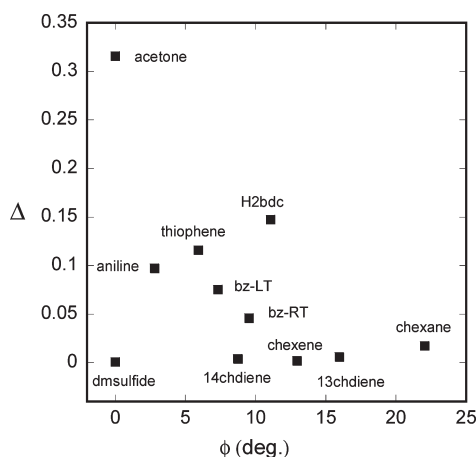


**Figure 4.** Deformations of the VO(bdc) framework loaded with different guest molecules.  $\Delta$  and  $\phi$  are measures of the breathing and the twisting deformation modes, respectively. dmsulfide, dimethylsulfide; H2bdc, 1,4-benzenedicarboxylic acid; bz, benzene; 14chdiene, 1,4-cyclohexadiene; 13chdiene, 1,3-cyclohexadiene; chexene, cyclohexene; chexane, cyclohexane.

the guests in the former. This is probably related to the different shapes and occupancies of the guest molecules in the two phases. The unit cell volume of **7** is larger than other phases mainly due to an expansion along the channel axis.

#### The Crystal Structure of [VO(bdc)](cyclohexane), **8**.

The absorbed cyclohexane molecules have a typical chair conformation. Their packing pattern and orientations are similar to the cyclohexene molecules in **7** (Figure 2). The shortest intermolecular  $\text{H}\cdots\text{C}$  distances between the cyclohexane guests is 3.41 Å, while the shortest distances from the hydrogen atoms of the cyclohexane molecules to the framework carbon and oxygen atoms are 3.09 Å and 3.00 Å, respectively. Therefore, they are held together mainly by van der Waals interactions. Compared to the other guest molecules, cyclohexane is the most voluminous but has the least extension along the six-ring plane. Therefore, the packed cyclohexane molecules have larger space requirement along the six-ring thickness direction and less space requirement along the six-ring plane. The requirement is met by the highest degree of bending of the channel walls, which also tends to maximize the number of van der Waals contacts between the guests and the host. The channel wall bending is accompanied by a cooperative rotation of the octahedral chains to release the strain.

**Breathing and Twisting, Two Different Framework Deformations.** Compared to the breathing deformation, the “twisting” deformation of the VO(bdc) framework observed above has less effect on the volume of the cell and on the aperture of the channels but does significantly vary the channel shape by changing the curvature of the channel walls. The magnitude of the breathing deformation is directly reflected in the ratio of the two channel diagonals measured between the metal atoms. For the pure breathing deformation observed on adsorption of acetone, this ratio changes from 14.00:16.07 in VO(bdc) to 10.21:18.41 in [VO(bdc)](acetone). In comparison, the ratio is 13.71:16.07 in [VO(bdc)](cyclohexane). The two deformation mechanisms are illustrated in Figure 3. If the VO(bdc) framework is considered an expanded  $\text{ReO}_3$  structure, the twisting deformation is similar to the  $a^0a^0c^+$  in-phase tilting deformation of the perovskite structures.<sup>57</sup>

The framework deformations observed to date for different guest molecules can be described by various combinations of the breathing and the twisting modes. In order to quantitatively characterize the deformation, we define the following parameters (see Figure 3):

$\Delta = |(b/c) - (b_0/c_0)|$ , variation of channel diagonal ratio ( $b/c$ ) from that of **2** with empty channels ( $b_0/c_0$ ), a measure of the breathing deformation

$\phi$ : angle between the zigzag  $-\text{V}=\text{O}-\text{V}=\text{O}-$  backbone planes of two neighboring octahedral chains, a measure of cooperative rotation of the octahedral chains and the twisting deformation. The variation of  $\Delta$  versus  $\phi$  for VO(bdc) is shown in Figure 4 for VO(bdc) frameworks loaded with different guest molecules. There is no substantial framework deformation upon the adsorption of dimethylsulfide that is found to be highly disordered in the VO(bdc) channels.<sup>37</sup> [VO(bdc)](acetone) shows a breathing deformation only, while phases **5–8** are dominated by twisting deformations. The other phases show different combinations of both breathing and twisting modes.

Since the two deformation modes are accompanied by different bending of the bdc ligands, we further define the following parameters in order to study the correlations

(57) Mitchell, R. H. *Perovskites Modern and Ancient*; Almaz Press: Thunderbay, Canada, 2002.

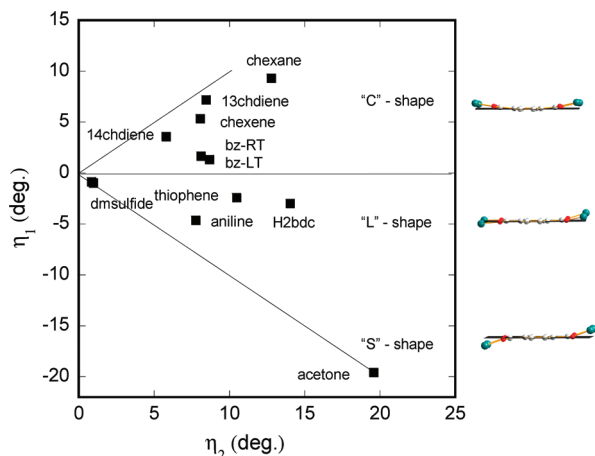


**Figure 5.** The relationship between  $\eta_1$  and  $\eta_2$  for the VO(bdc) framework loaded with different guest molecules, showing that the channel walls bend differently for different deformation modes. Abbreviations are the same as in Figure 4.

between the deformation mode and shapes of channel walls:

$\eta_1, \eta_2$ : bending angles of the (V1)<sub>2</sub>–bdc–(V2)<sub>2</sub> channel wall, defined as the angle between the line through the two benzene C atoms on the bdc long axis and the best plane fitting the two V–O bonds on V1 and V2 respectively,  $|\eta_1| \geq |\eta_2|$ . If the V atoms are all on the same side of the bdc plane, both  $\eta_1$  and  $\eta_2$  are positive; otherwise,  $\eta_1$  is positive and  $\eta_2$  is negative.

$\varepsilon_1, \varepsilon_2$ : hinge angles of the (V1)<sub>2</sub>–bdc–(V2)<sub>2</sub> channel wall, defined as the angle between the carboxylate plane and the best plane fitting the two V–O bonds on V1 and V2, respectively,  $|\varepsilon_1| \geq |\varepsilon_2|$ . If the V atoms are all on the same side of the bdc plane, both  $\varepsilon_1$  and  $\varepsilon_2$  are positive; otherwise,  $\varepsilon_1$  is positive and  $\varepsilon_2$  is negative.

$\psi$ : bending angle of the bdc ligand, the angle between the two C–C single bonds of bdc. As shown in Figure 5 where  $\eta_1$  is plotted against  $\eta_2$ , the channel walls bend differently for the breathing and twisting modes. For breathing, the wall bends to an “S” shape because the V atoms on the two edges of the wall shift to the opposite sides of the bdc plane, while for twisting they tend to shift to the same side so that the wall bends to a “C” shape. Some of the phases with combined deformation of both breathing and twisting modes have walls approaching an “L” shape.

Assuming the octahedral chains are rigid, the rotation angle  $\phi$  of the octahedral chains is expected to be equal to the sum of the bending angles  $\eta_1 + \eta_2$ . As shown in Figure 6, this is indeed the case for most of the phases. In fact, even for the most twisted phase [VO(bdc)](cyclohexane), **8**, the VO<sub>6</sub> octahedron changes very little from that of VO(bdc), **2**. The maximum difference in corresponding O–V–O angles between the two frameworks is less than 1°. The bending of the V–bdc–V channel walls consists of two parts: the hinging angles and the bending of the bdc ligand. As shown in Figure 7, the net bending of the channel walls  $\eta_1 + \eta_2$  is approximately equal to the net hinge angles  $\varepsilon_1 + \varepsilon_2$  plus the bending angle of the bdc ligand  $\psi$ . Bending of the bdc ligand  $\psi$  is somewhat less than the net hinge angles  $\varepsilon_1 + \varepsilon_2$ . Both increase as the degree of twisting increases (Figure 7).

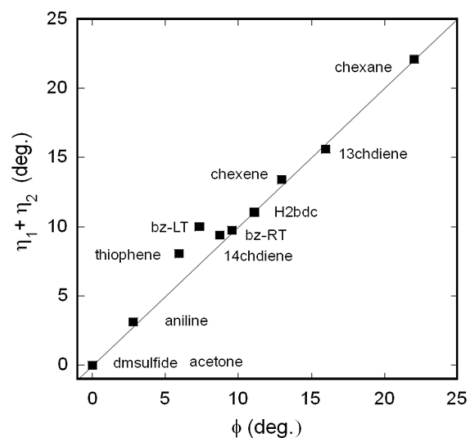


**Figure 6.** Correlation between the cooperative rotation of the octahedral chains and the bending of the channel walls of the VO(bdc) framework loaded with different guest molecules. Abbreviations are the same as in Figure 4.

We may attempt to relate the observed structural deformations to the relative energies of the various frameworks. Table 2 lists relative single point energies (kcal/mol) from our VASP calculations of the empty VO(bdc) frameworks (after “removal” of the different guest molecules) on the basis of results from the single crystal X-ray diffraction data. The energy of VO(bdc), **2**, without guest loading was taken as the reference (i.e., energy = 0.0 kcal/mol).

The relative energies of five of the structures, including that of the empty framework, fall within about 2 kcal/mol. Such small differences are not likely to be significant. Three other structures differ by less than 10 kcal/mol from the one with the lowest energy, while the framework for the acetone inclusion compound is 26.2 kcal/mol higher in energy. These results may be correlated to some degree with the details of the framework distortions observed in the single crystal X-ray diffraction data, and described above. Reference to Figure 4, where the breathing ( $\Delta$ ) and twisting deformations ( $\phi$ ) of the different framework structures are displayed, reveals that five of the structures found to have the lowest energies (dms, aniline, thiophene, benzene LT, and the empty framework) roughly fall on a diagonal with modest values of  $\Delta$  and  $\phi$ . The other structures, which deviate in energy by more significant amounts, either exhibit a large breathing deformation (acetone) with no twisting deformation or (1,4-cyclohexadiene, cyclohexene, 1,3-cyclohexadiene, and cyclohexane) show little or no breathing deformation accompanied by various degrees of twisting. Figure 5 shows that the latter frameworks are those closer to a C shape, while the acetone framework is one with a pronounced S shape. The low energy structures in turn have a framework closest to an L shape.

In an effort to separate the effects of structural distortions from that of the binding of guest molecules, we obtained estimates of the binding energies for three host/guest systems listed in Table 3. These are taken to be the difference in the single-point energies (based on experimental crystal structures) of the framework including guests to the sum of energies of the empty framework and the guests themselves (in the configuration found in the framework). It should be noted, however, that the

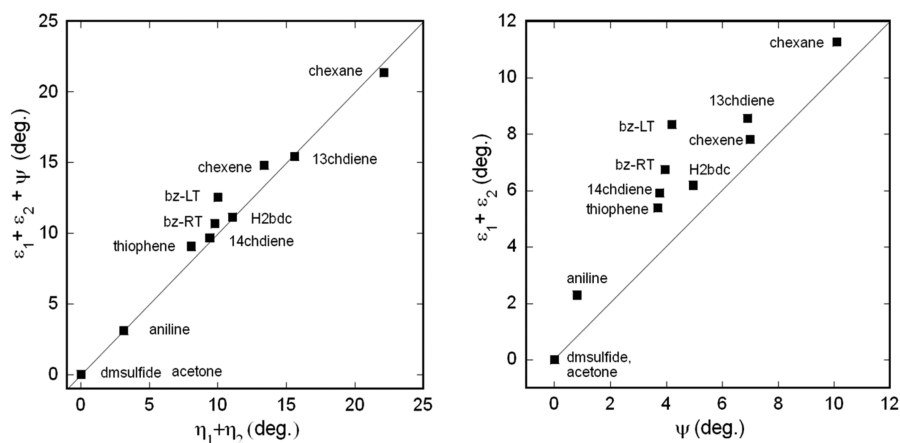


**Figure 7.** Left: The net bending of the channel walls ( $\eta_1 + \eta_2$ ), which is approximately equal to the net hinge angles ( $\epsilon_1 + \epsilon_2$ ) plus the bending angle of the bdc ligand ( $\psi$ ). Right: Correlation between  $\epsilon_1 + \epsilon_2$  and  $\psi$  of the VO(bdc) framework loaded with different guest molecules. Abbreviations are the same as in Figure 4.

**Table 2.** Relative Single Point Energies of the Empty VO(bdc) Framework Structures with the Respective Guest Molecules Removed on the Basis of Single Crystal X-Ray Diffraction Data<sup>a</sup>

framework	relative energy (kcal/mol)
[VO(bdc)](cyclohexene)	−7.6
[VO(bdc)](dms)	−2.1
[VO(bdc)](aniline)	−1.2
[VO(bdc)](thiophene)	−0.54
[VO(bdc)](benzene)-LT	−0.47
VO(bdc)	0.0
[VO(bdc)](1,3-cyclohexadiene)	4.4
[VO(bdc)](1,4-cyclohexadiene)	5.5
[VO(bdc)](cyclohexane)	15.2
[VO(bdc)](acetone)	26.2

<sup>a</sup> The energy of VO(bdc) before loading guests was taken as the reference (i.e. energy = 0.0 kcal/mol).

values obtained in this manner are likely to underestimate binding energies of the guest molecules, as this type of calculation does not adequately account for dispersion forces, as such corrections are not currently supported in VASP. The values for the three systems investigated in this manner were all between 4 and 5 kcal/mol, largely independent from the extent to which the host framework was distorted. This result suggests that additional factors play a role in the distortion of the framework upon the inclusion of guest molecules, which could be of a kinetic nature during the synthesis.

In an effort to investigate this point further, and to understand why the empty framework structure is not the one with the lowest energy, we performed full geometry relaxation (atomic positions and, subsequently the cell parameters) of five of the structures, VO(bdc), [VO(bdc)](dms), [VO(bdc)](thiophene), [VO(bdc)](cyclohexane), and [VO(bdc)](acetone), without the presence of guest molecules. In all three cases, the structures became more distorted, decreased in cell volume, and reached minimum energies more than 75 kcal/mol lower than those of the corresponding empty framework but had not converged after 500 optimization steps. Perhaps the most noteworthy aspect of the relaxed structures is that in all cases the bdc linker turns more inclined to the channel axis (Figure 8), akin to what is the case for MOF-5, for example. Dynamic flips of the bdc

**Table 3.** Estimate of the Binding Energies of Guest Molecules for Three Framework Structures (See Text)

phase	binding energy (kcal/mol)
[VO(bdc)](benzene)-LT	4.1
[VO(bdc)](thiophene)	4.5
[VO(bdc)](acetone)	4.9

phenyl rings in VO(bdc) and MIL-53(Cr) were unveiled using the <sup>2</sup>H NMR method most recently.<sup>58</sup>

We may add that it is the VO(bdc) framework which we found to have the lowest energy of the five structures after relaxation in the manner described above. It is also no surprise, of course, that these frameworks will reduce in volume in the absence of guest molecules and may, in fact, change shape and ultimately collapse. The relative energies of the synthesized frameworks without guest molecules must therefore be treated with caution.

As discussed in previous sections, the twisting deformations are mainly related to adaption of the framework to the packing of the guests so that the van der Waals interactions between the host and the guest can be maximized. In the case of strong breathing deformations, pronounced interactions between guests and the octahedral chains of the framework can be identified. In [VO(bdc)](acetone), dipole–dipole interactions between the acetone molecules and the carboxylate groups of the framework were observed, which tend to pull a pair of opposite octahedral chains to the channel axis. Similarly, in [Al(OH)(bdc)](H<sub>2</sub>O), which shows a very large breathing deformation, significant hydrogen bonding between the guest water molecules and the framework oxygen atoms was observed.<sup>59</sup> The adsorption-induced stress exerted on the host framework may act as a stimulus that triggers breathing transitions.<sup>60</sup>

The deformation parameters defined in the last section can also be used to help describe framework deformation of other members of the MIL-47 and MIL-53 families. In

(58) Kolokolov Daniil, I.; Jobic, H.; Stepanov Alexander, G.; Guillemin, V.; Devic, T.; Serre, C.; Férey, G. *Angew. Chem., Int. Ed. Engl.* **2010**, *49*, 4791–4.

(59) Loiseau, T.; Serre, C.; Huguenard, C.; Fink, G.; Taulelle, F.; Henry, M.; Bataille, T.; Férey, G. *Chem.—Eur. J.* **2004**, *10*, 1373–1382.

(60) Neimark, A. V.; Coudert, F.-X.; Boutin, A.; Fuchs, A. H. *J. Phys. Chem. Lett.* **2009**, *1*, 445–449.

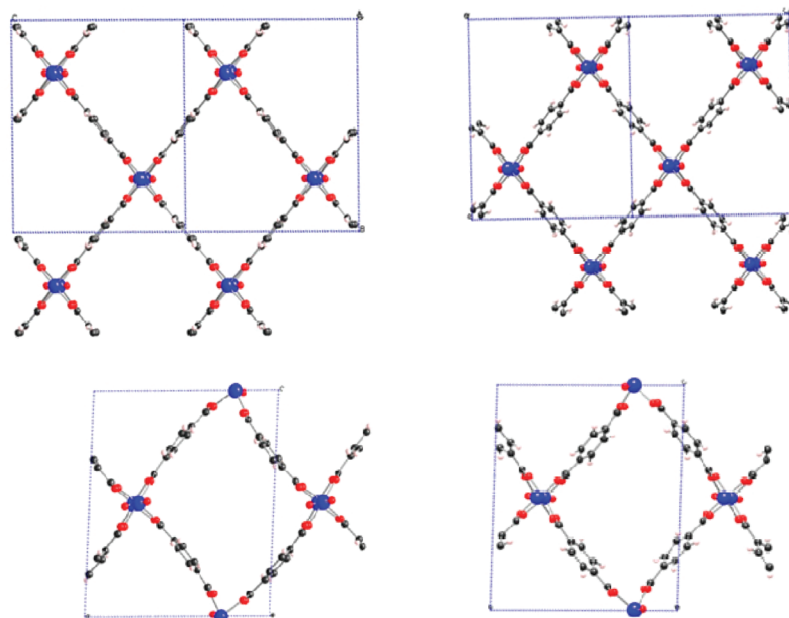


**Figure 8.** (a) VO(bdc), diffraction data (top left), relaxed (top right). (b). [VO(bdc)](cyclohexane) cell crystal structure (bottom left), relaxed (bottom right).

some monoclinic phases such as [Al(OH)(bdc)]-LT<sup>61</sup> and [Fe(OH)(bdc)](pyridine),<sup>12</sup> neighboring MO<sub>6</sub> octahedra of each individual chain are slightly rotated relative to each other, usually coupled with increased inclination of the bdc ligands toward the channel axis. The breathing or twisting deformation parameters of such frameworks can also be determined by cooperating translation or rotation of neighboring octahedral chains. In the system [Al(OH)(bdc)](pyridine)<sub>x</sub>, depending on the value of *x*, the guest packing can be switched between two different patterns, and accordingly, the framework shows different deformation modes. For *x* = 1, the pyridine molecules are packed in two columns in each channel very similarly to benzene molecules in [VO(bdc)](benzene)-LT, and the framework shows mainly a twisting deformation. If *x* decreases to 0.8, the pyridine molecules are packed perpendicular to the channel axis in a single column, and the framework is deformed in the breathing mode. In contrast, for the system [Ga(OH,F)(bdc)](pyridine)<sub>x</sub>, when *x* changes from 1 to 0.85, the framework shows increased breathing deformation but no twisting, although the packing of the guest pyridine molecules changes dramatically.<sup>14</sup> These observations suggest that both breathing and twisting deformations should be considered in studies of the adsorption of various molecules, especially by computer simulations.

(61) Liu, Y.; Her, J.-H.; Dailly, A.; Ramirez-Cuesta, A. J.; Neumann, D. A.; Brown, C. M. *J. Am. Chem. Soc.* **2008**, *130*, 11813–11818.

## Conclusion

All of the six-ring guest molecules show a high degree of ordering inside the channels of VO(bdc). The interactions between the guests and the host framework are dominated by van der Waals bonding; therefore, the packing of the guest molecules adopts patterns that tend to maximize the van der Waals contacts. The six-ring molecules are all packed in two columns in each channel, either in herringbone or close to parallel patterns. Such packing is not compatible with the space group symmetry *Pnma* of the VO(bdc) framework, and all of the phases have the noncentrosymmetric space group *P2<sub>1</sub>2<sub>1</sub>2<sub>1</sub>*. The VO(bdc) framework deforms so that it closely fits the shape and thickness changes of the double columns of the guest molecules. In addition to the well studied breathing deformation, the phases reported here show a much more pronounced twisting deformation, associated with cooperative rotations of the octahedral chains accompanied by bending of the bdc ligand.

**Acknowledgment.** We (X.W., L.L., A.J.J.) thank the R. A. Welch Foundation (#E-0024), NHARP—Chemistry 003652-0092-2007, and NSF DMR-0706072 for support of this work. One of us (J.E.) wishes to acknowledge support from the Office of Energy Efficiency and Renewable Energy, U.S. DOE.

**Supporting Information Available:** Crystallographic information files in CIF format. This material is available free of charge via the Internet at <http://pubs.acs.org>.